



Contents lists available at ScienceDirect

Chinese Chemical Letters

journal homepage: www.elsevier.com/locate/cclet

Original article

Template-directed synthesis of pyridazine-containing tetracationic cyclophane for construction of [2]rotaxane

Qi Qiu-Sheng Fang, Ling Chen*, Qing-Yan Liu

Department College of Chemistry and Chemical Engineering, Key Laboratory of Functional Small Organic Molecules, Ministry of Education, Institution Jiangxi Normal University, Nanchang 330022, China

ARTICLE INFO

Article history:

Received 13 October 2016
Received in revised form 9 November 2016
Accepted 25 November 2016
Available online xxx

Keywords:

Tetracationic cyclophane
Template effect
Inclusion complex
 π -Stacking
Rotaxane

ABSTRACT

Benefiting from its bent molecular structure, 3,6-pyridazinyl contained tetracationic cyclophane (**1**) is synthesized by template-directed method with high isolated yield up to 92%. This template-directed strategy is further utilized to efficiently construct [2]rotaxane.

© 2016 Ling Chen. Chinese Chemical Society and Institute of Materia Medica, Chinese Academy of Medical Sciences. Published by Elsevier B.V. All rights reserved.

1. Introduction

Recently, great progress has been achieved in the design and synthesis of functionalized molecular machines. In this regard, interlocked molecules as promising candidates have been received much attention and inventive applications in catalysts, sensors, photoelectronics and metamaterials [1]. One attractive approach is to exploit new molecular recognition leading to highly efficient synthesis of interlocked structures such as rotaxanes and catenanes, and molecular devices [2]. Of the potential classes of macrocyclic compounds for use in interlocked molecules and molecular devices, tetracationic cyclophanes are often employed because of their favorable electronic, redox property and diverse binding ability. These host molecules usually possess a cavity around with two π -deficient extended planes and two aromatic linkers, in which a wide range of π -efficient guest molecules can be bound. Well-defined variations [3] on the π -deficient and aromatic linkers can dramatically influence the supramolecular behaviors. Although lots of classic structures have been reported, the design and synthesis of new cationic cyclophanes are still important to be exploited in supramolecular chemistry [4]. The desired variation may be executed by introducing a variety of heterocycles as π -moiety. Heterocycles not only endow the cyclophanes with

versatile cavity size, but also bring about the variable conformation due to the low symmetry of most heterocycles [3,5].

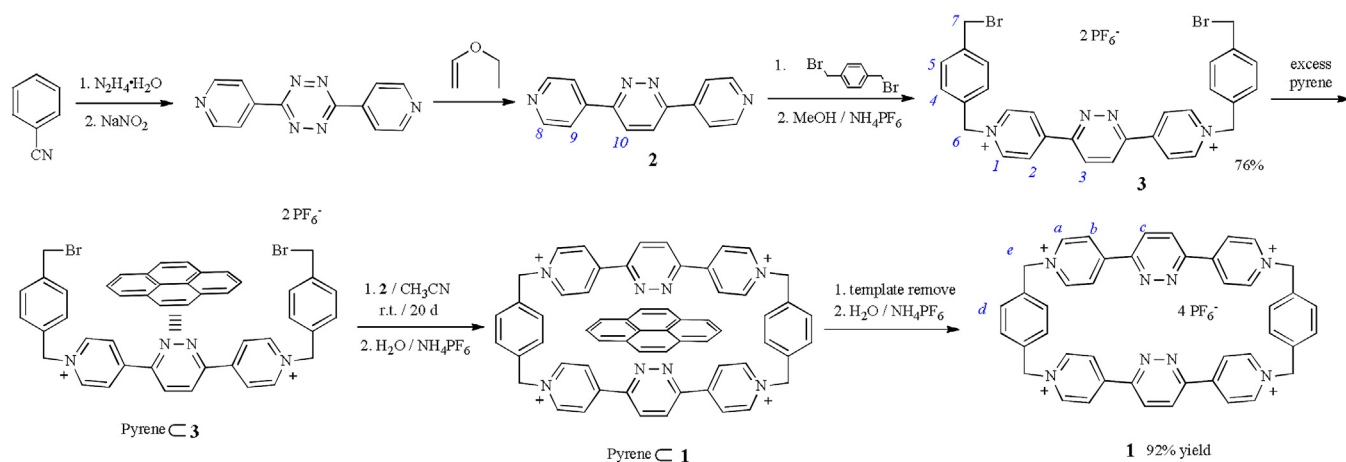
This realization prompted the design of new tetracationic cyclophane that utilizes the heterocycle pyridazine as part of π -deficient moiety. Here, we represented a novel tetracationic cyclophane (**1**) consisted of two 3,6-bis(4-pyridinium)pyridazine and two 1,4-bis(methylene)phenylene. The new host **1** has a moderate bent geometry arose from the low symmetry of pyridazine rings. **1** shows ideal template effect which leads to high macrocyclization yield up to 92% in presence of appropriate template. Since template methods are often employed to make macrocyclic molecules and interlocked molecules, the synthesis of **1** was extended to made [2]rotaxane with excellent yield. As detailed below, a series of experiments were carried out to investigate the molecular recognition and template effect by NMR, UV spectra, X-ray crystallography, and synthesis of a [2]rotaxane.

2. Results and discussion

Synthetic routes for **1** are shown in Scheme 1. The starting precursor 3,6-pyridazyl extended bipyridine (**2**) was prepared by well-described [4+2] cycloaddition reaction, executed by reacting 4-cyanopyridine with hydrazine hydrate to obtain 3,6-di-4-pyridyl-1,2,4,5-tetrazine, then [4+2] cycloaddition was carried out by reacting tetrazine with ethyl vinyl ether [6]. And the addition product bipyridine **2** is easily obtained on one hundred gram scale. Then, macrocyclization of **1** was proceeded in two steps

* Corresponding author.

E-mail address: chenlingjxnu@163.com (L. Chen).

Scheme 1. Two-step synthesis of **1**.

from **2** using excess pyrene as template, which closely resembled the other tetracationic cyclophanes reported before. Using pyrene as template, bisbromomethyl[bis-*p*-benzyl-4,4'-(3,6-pyridazinyl)-bispyridine] bis(hexafluorophosphate) (**3**) was reacted with equimolar amounts of **2** in dry MeCN at room temperature for 20 days. After removal of template and counterion exchange, **1** was isolated as tetrakis(hexafluorophosphate) salt with yield up to 92%. In contrary, the isolated yield dropped to only 17% without pyrene template. These results indicate that appropriate template such as pyrene is a key factor for the efficient synthesis of **1**. It is also found that such example of nearly quantitative macrocyclization is uneasy to be achieved synthetically in supramolecular chemistry [7], and the newly synthesized **1** allows us to explore it as a useful host for molecular recognition and interlocked molecules.

At the outset, the macrocyclization process of **1** with excess pyrene as template was investigated by 1H NMR spectroscopy. As shown in Fig. 1a, upon addition of excess pyrene to an equimolar mixture of **2** and **3** in CD_3CN in a NMR tube, the signals for H_1 , H_2

and H_3 on **3** were shifted upfield, indicating that **3** associated with pyrene to form a π -donor-acceptor complex with π -electron shielding of the face-to-face oriented aromatic rings (Fig. S12 in Supporting information). Then, 1H NMR spectrum was recorded after 4 days (Fig. 1b), showing several new signals which was assigned to the protons in pyrene \subset **1** complex. The relative intensities of new signals suggested about 53% of the starting materials had been converted to pyrene complex as pyrene \subset **1**. During a reaction period between 5 min to 20 days, the signals corresponding to **2** and **3** disappeared gradually, and those for the pyrene \subset **1** complex appeared accordingly. The reaction was finally completed after about 20 days, which exhibited only five groups of proton signals with respect to pyrene \subset **1** complex, suggesting that **1** was almost exclusively formed in solution (H_{a-e}). In comparison, the 1H NMR spectra of equimolar-mixed of **2** and **3** without pyrene template was recorded at the same experimental condition (Fig. S13 in Supporting information). Although the proton signals corresponding to **2** and **3** disappeared after 20 days, only several

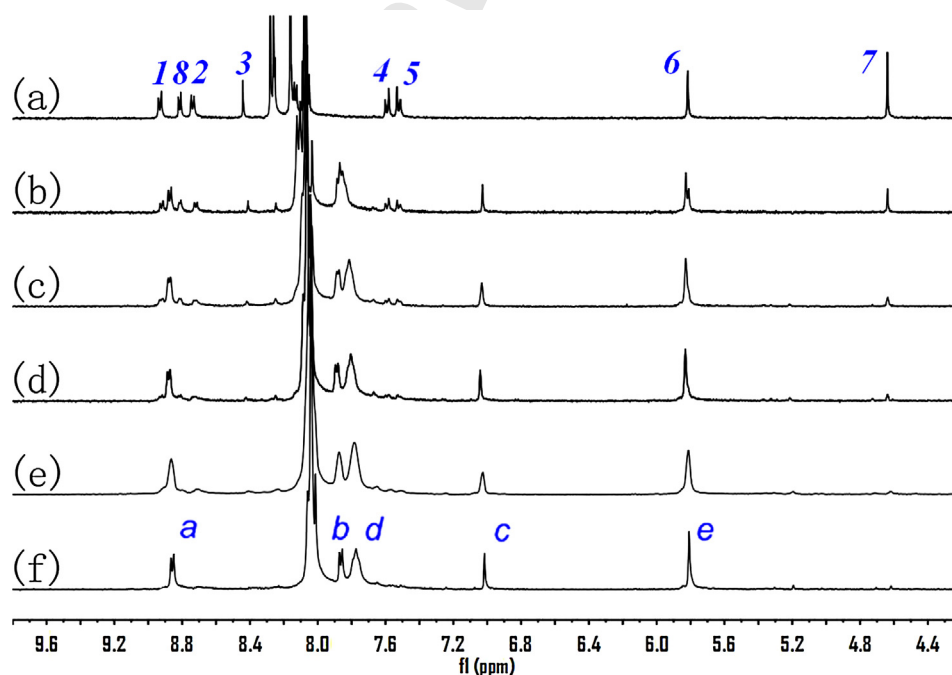


Fig. 1. Partial 1H NMR spectra of a mixture containing **2** (3 mmol/L), **3** (3 mmol/L) and pyrene (15 mmol/L) in CD_3CN at 25 °C for (a) 5 min, (b) 4 days, (c) 8 days, (d) 11 days, (e) 15 days and (f) 20 days.

Table 1

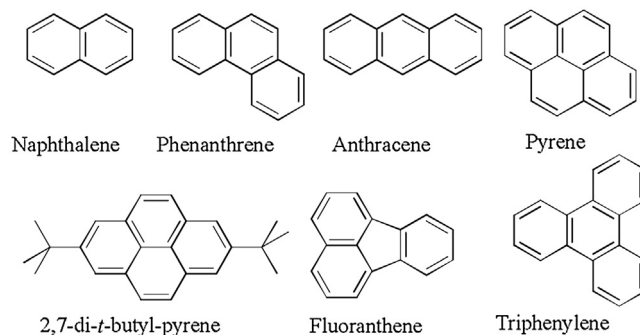
The binding parameters of PAHs toward with **1** determined by UV–vis spectroscopy titration.

PAHs	π -electron count	ΔG (kJ/mol)	K_a (L/mol)
Naphthalene	10	9.14	40
Phenanthrene	14	18.13	1.50×10^2
Anthracene	14	16.65	8.27×10^2
Pyrene	16	20.67	4.18×10^3
2,7-Di- <i>tert</i> -butyl-pyrene	16	15.46	5.11×10^2
Fluoranthene	16	21.24	5.27×10^3
Triphenylene	18	23.37	1.24×10^4

weak peaks of **1** could be observed, indicative of the macrocyclization process occurred in low efficiency.

Subsequently, seven polycyclic aromatic hydrocarbons (Fig. 2, PAHs) guests varying from two to four rings were selected to study their capability for the forming inclusion complexes with **1** by UV spectroscopy titration [8]. As shown in Table 1, the association constants (K_a) for the seven guests with **1** ranging from 40 L/mol for naphthalene to 1.24×10^4 L/mol for triphenylene. The two guests pyrene and fluoranthene which have similar molecular size and π -electron count displayed very close binding strength toward **1**. On contrary, although pyrene and 2,7-di-*tert*-butyl-pyrene have the same π -electron count and aromatic core, the K_a value for 2,7-di-*tert*-butyl-pyrene is far smaller than that for pyrene. This could be attributed to steric hindrance of *tert*-butyl group that seriously restricts the penetration of pyrene plane from the 1,6- or 2,7-orientation, the restricted π -stacking therefore drop the binding strength of 2,7-di-*tert*-butyl-pyrene.

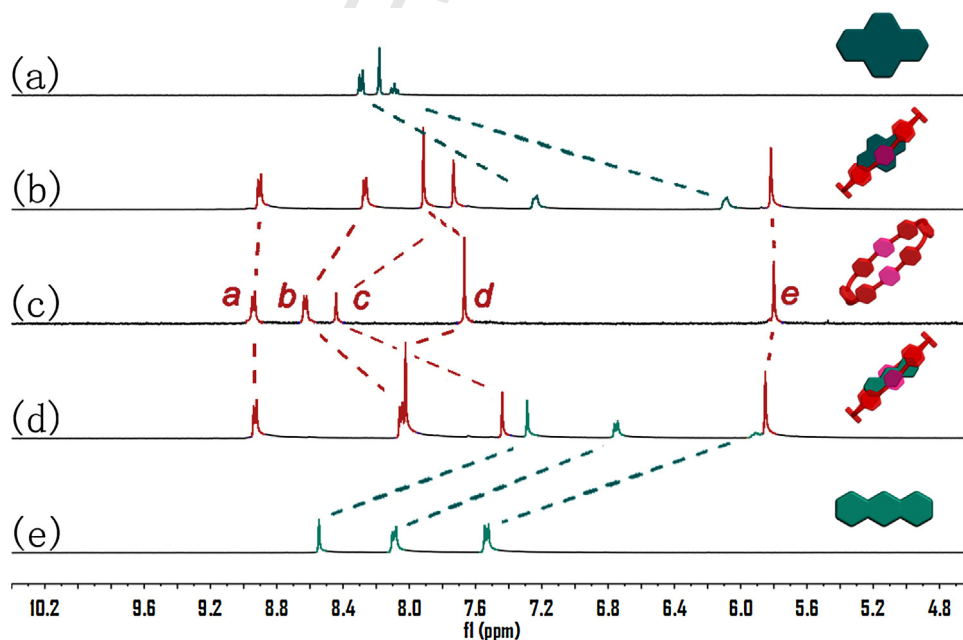
The molecular binding of pyrene and anthracene by **1** was selected to investigate in CD₃CN by ¹H NMR spectroscopy. As can be seen in Fig. 3, the proton signals of two complexes (pyrene \subset **1** and anthracene \subset **1**) exhibited fast-exchange equilibrium on ¹H NMR time scale. The two complexes displayed remarkable upfield shifts for almost all of the aromatic protons on both the host and guests except the slight upfield shifts for H_a, whereas there was only a significant downfield shift corresponding to the resonances associated with the *para*-xylylene protons (H_a). These upfield shifts were originated from mutual π -electron shielding of

**Fig. 2.** Chemical structures of seven PAHs.

face-to-face oriented π -stacking [9], while the small shift values of H_a indicate that the stacking mainly occurs between pyrene/anthracene and the central of pyridazine-bridged bipyridinium. Moreover, the significant downfield shift for the *para*-xylylene (C₆H₄) protons on **1** could be related to the C–H $\cdots\pi$ interaction between the hydrogen atoms on guests and *para*-xylylene plane. From the ¹H NMR spectrum it is clearly deduced that the noncovalent interaction between aromatic guest and **1** is mainly consisted of face-to-face and edge-to-face π -stacking interaction. Moreover, the complexation of pyrene \subset **1** and anthracene \subset **1** was also proved by ESI-MS experiments. As expected, the peaks at *m/z* 219.60, and 213.60 could be clearly assigned to [(**1**⁴⁺ + pyrene)/4]⁺ and [(**1**⁴⁺ + anthracene)/4]⁺, respectively.

Next, in order to probe the structural characteristics of **1** upon binding with PAHs, two inclusion complexes anthracene \subset **1** and pyrene \subset **1** were investigated in the solid state by single crystal X-ray diffraction. As shown in Fig. 4, both the two guests are bound in the cavity by face-to-face and edge-to-face π -stacking interaction. The pyridazine rings locate in the central of bipyridiniums moieties with almost planar conformation, bringing two geometrical characteristics.

- (1) The pyridazine bridged bipyridinium has bent geometry. Nitrogen atoms have smaller radius than carbon atoms, and

**Fig. 3.** Partial ¹H NMR spectra of (a) pyrene, (b) pyrene \subset **1** complex, (c) **1**, (d) anthracene \subset **1** complex, (e) anthracene in CD₃CN at 25 °C, respectively (400 MHz, [pyrene]=[**1**]=[anthracene]=4 mmol/L).

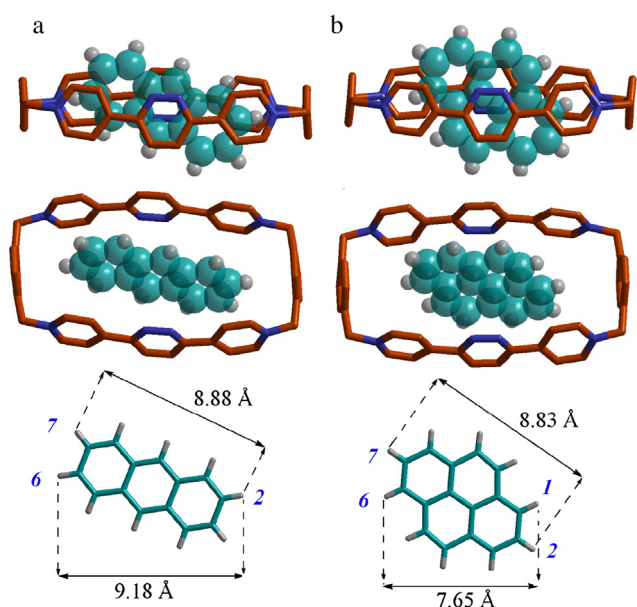
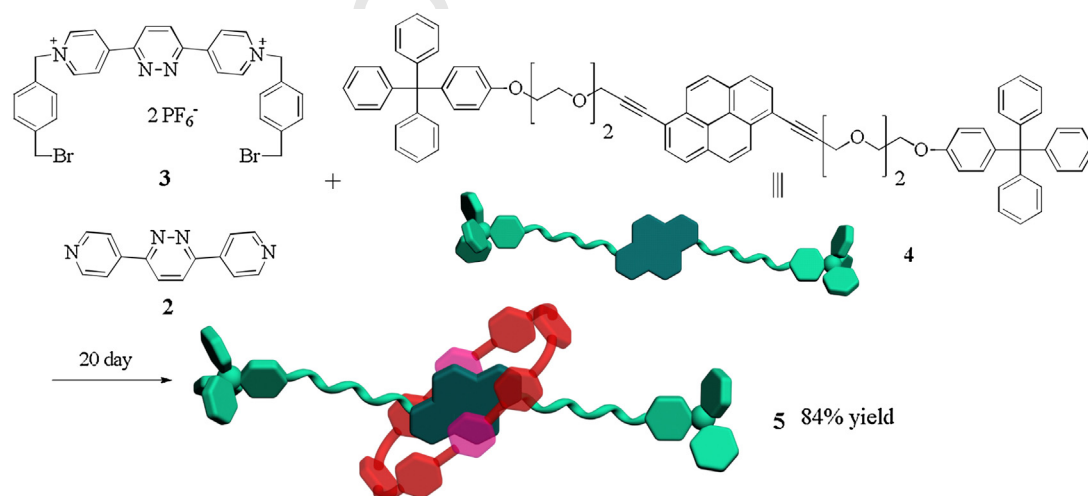


Fig. 4. Crystal structure and molecular size of the complexes for **1** with anthracene (a) and pyrene (b). Solvent molecules, counter ions and partial hydrogen atoms are omitted for clarity.

thus the sp^2 bond angles on the neighboring 3,6-position of pyridazine rings deviate from the idealized 120° . The bond nearby the two nitrogen atoms incline to the nitrogen atoms for about 5° , and the plane of 3,6-pyridazine-bridged bipyridinium is bent totally for about 12° (Fig. 4). It is well-known that tetracationic cyclophanes have a certain degree of inner strain due to the bond angle restriction [10]. Bent aromatic moieties of cationic cyclophane can usually induce lower bond angle strain and modified the synthetic yield [3e,4]. Some examples with imidazole groups even display flexible conformation and an ability to alter ring shape to accommodate different guests [11]. Here the moderate bent geometry in tetracationic cyclophane **1** could relax the inner bond strain to a certain degree while the main binding ability of **1** toward aromatic guests is withheld. This provides modest encouragement and motivation to the trend of macrocyclic formation, and eventually results in a highly efficient template-directed macrocyclization.

(2) The orientation of the two guests bound in the cavity is quite distinguishable. Indeed, the $C-H \cdots \pi$ geometry of both two complexes is identically parallel to the bipyridinium moieties. However, in the crystal structure of anthracene \subset **1**, the most distant 2,6-H atom being 9.18 Å apart to each other get close contact of $C-H \cdots \pi$ with *para*-phenylene, the $H-\pi$ distance is only 2.60 Å. In the case of pyrene \subset **1**, the comparable $C-H \cdots \pi$ contact do not take place on the most distant 2,7-H atom ($d_{H_2-H_7} = 8.83$ Å) but the 1,6-H atom ($d_{H_1-H_6} = 7.65$ Å) instead with $H-\pi$ distance of 3.32 Å (Fig. 4). This unexpected phenomenon indicates that the noncovalent interaction for anthracene \subset **1** has more $C-H \cdots \pi$ portion than that for pyrene \subset **1**, which can also be explained by the bent structure of pyridazine-bridged bipyridinium. Each of the two pyridazine moieties were pushed away from the central of the cavity for 1.18 Å due to the bent geometry, which subsequently induce the short and wide pyrene guest to turn to the pyridazines and obtain more π -stacking surface area. In comparison, anthracene with long and narrow size has less stacked π -surface area and incline to locate in the cavity along 1,6-orientation to get close contact of $C-H \cdots \pi$ as much as possible.

Above experiments revealed that the bent geometry of macrocyclic molecule **1** significantly influences the molecular recognition and template effect, it is important to extend this efficient macrocyclization strategy to synthesize interlocked molecules like rotaxane [12]. Favorable synthetic yield is expectable to be achieved if appropriate axles with pyrene core is selected, which is important in rotaxane synthesis. A tailor-made axle **4** possessing one pyrene binding site and two tetraphenyl stoppers was synthesized by Sonogashira reaction. The axle **4** has limited solubility in acetonitrile (about 3 mmol/L) and good solubility in chloroform. By mixing the precursors **2**, **3**, and **4** in CH_3CN for 20 days at room temperature, [2]rotaxane **5** was obtained with 84% isolated yield at last (Scheme 2). 1H NMR spectra demonstrated that the reaction has obviously progressed after 0.5 day, and after 20 days there are still some unreacted starting material, which might be the limited solubility of axle **4** in CD_3CN . The 1H NMR spectra of purified **5** showed the binding and blocking of [2]rotaxane were successfully achieved, as discerned from the appearance of signals for **1** (Fig. 5), further corroborating that **1** could act as an useful macrocyclic host for the template-directed synthesis of interlocked molecules.



Scheme 2. Synthesis of [2]rotaxane **5**.

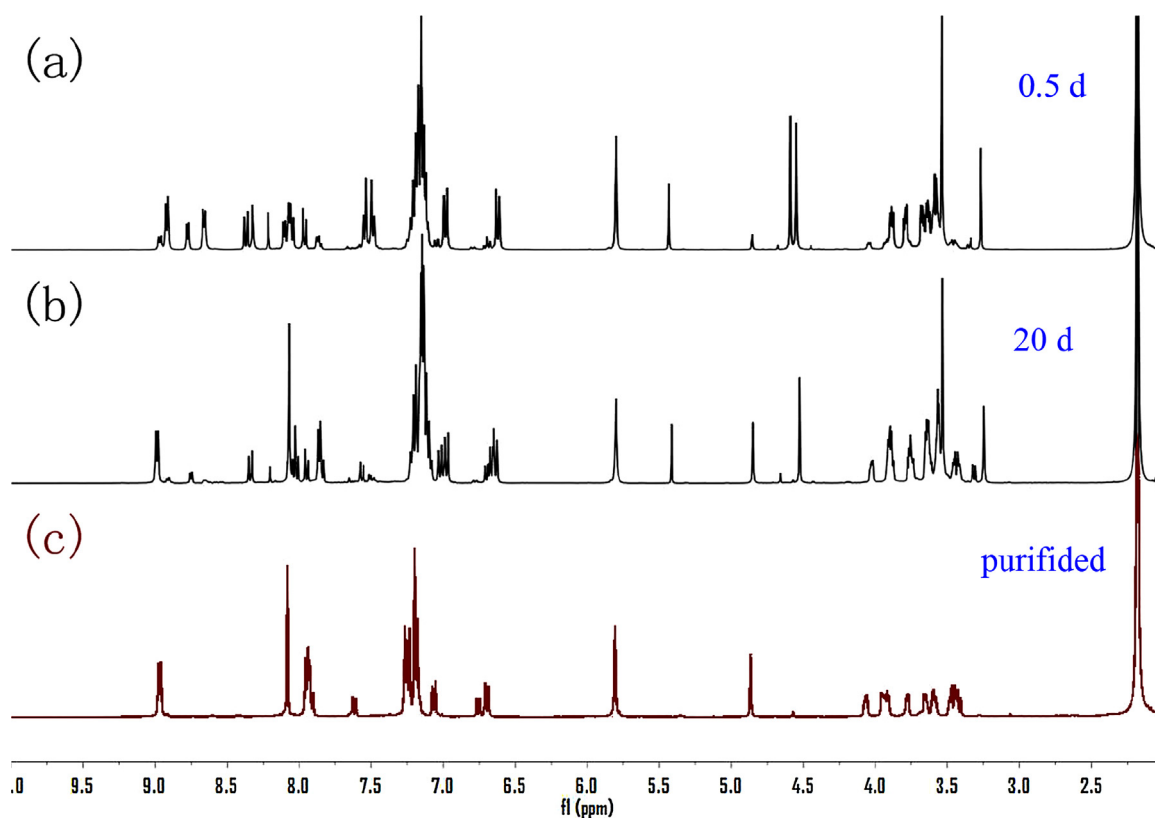


Fig. 5. ^1H NMR spectra of a mixture containing **2**, **3**, and **4** for (a) 0.5 day; (b) 20 days; (c) 20 days followed with purification.

3. Conclusion

In conclusion, this work has demonstrated the introduction of pyridazine as part of π -moiety can dramatically improve the template effect of the tetracationic cyclophane **1**, which showed excellent yield in macrocyclization and synthesis of [2]rotaxane. This host-guest system ideal template effect can act as significant candidate in the construction of more advanced molecular machines.

4. Experimental

4.1. General

All chemicals were commercially available unless otherwise noted. ^1H NMR spectra were performed on a Bruker AV400 spectrometer. Mass spectra were performed on Agilent 6520 Q-TOF LC/MS (ESI). Absorption spectra were recorded on a Hitachi U-3310 UV-vis spectrometer. The X-ray intensity data for pyrene-**1** and anthracene-**1** were collected on a Rigaku MM-007 rotating anode diffractometer equipped with a Saturn 724 CCD Area Detector System, using monochromated Mo-K α ($\lambda = 0.71073 \text{ \AA}$) radiation at $T = 296(2) \text{ K}$.

4.2. Synthesis of **3**

α,α' -Dibromo-*p*-xylene (10.0 g, 37.9 mmol) was added to MeCN (50 mL) and refluxed under N_2 . After all the solid dissolved, **1** (1.0 g, 4.3 mmol) in hot MeCN (250 mL) was added slowly over 3 h. Then the mixture was reflux for further 12 h and yellow precipitate formed. The yellow solid was collected by filtration, washed with MeCN and CH_2Cl_2 , and then dissolved in cold ($\leq 25^\circ\text{C}$) MeOH ($\sim 2 \text{ L}$). Addition of NH_4PF_6 (1.0 g) in 50 mL H_2O and then H_2O ($\sim 2 \text{ L}$) resulted in **3** as yellow precipitate. The yellow precipitate was

collected and column chromatographed over a shot silica gel using MeCN to obtain pure **3** as a yellow solid (3.1 g, 82%). ^1H NMR (400 MHz, CD_3CN): δ 8.96 (d, 4H, $J = 6.9 \text{ Hz}$), 8.84 (d, 4H, $J = 6.9 \text{ Hz}$), 8.60 (s, 2H), 7.59 (d, 4H, $J = 8.2 \text{ Hz}$), 7.56 (m, 4H), 5.83 (s, 4H), 4.64 (s, 4H). ^{13}C NMR (100 MHz, CD_3CN): δ 151.32 (s), 145.36 (s), 140.31 (s), 132.93 (s), 130.20 (s), 129.70 (s), 127.55 (s), 126.11 (d, $J = 7.8 \text{ Hz}$), 117.42 (s), 63.94 (s), 32.62 (s). HRMS (ESI): m/z calcd. for $(\text{C}_{30}\text{H}_{26}\text{Br}_2\text{F}_6\text{N}_4\text{P})^+ [\text{M}-\text{PF}_6]^+$, 745.0165; found, 745.0158.

4.3. Synthesis of **1**

3 (1.20 g, 1.34 mmol), **2** (0.315 g, 1.36 mmol), and the template pyrene (1.20 mg, 5.93 mmol) to dry MeCN (500 mL) and stirring under N_2 at room temperature for 15 days. Then tetraethylammonium bromide was added to get the inclusion complexes pyrene-**1** (bromide) as red precipitate. The precipitate was collected by filtration, washed with MeCN and dissolved in water (1 L). Then the aqueous solution was extracted 30 times with CH_2Cl_2 /toluene ($v/v = 1:1$, 100 mL per extraction), while the color of the solution change from red-orange to white. Then NH_4PF_6 (1.0 g) in 50 mL H_2O was added and precipitate was formed and collected by filtration to obtain gray yellow crude product (1.60 g, 95%). The pure **1** was obtained by further refluxing in CHCl_3 /acetone ($v/v = 2:1$, 100 mL) for 1 h. After cooling down, the precipitate was collected by filtration and then dried in vacuum to yield the product as gray yellow solid (1.55 g, 92%) which was pure after examination of ^1H NMR. ^1H NMR (400 MHz, CD_3CN): δ 8.95 (d, 4H, $J = 6.9 \text{ Hz}$), 8.64 (d, 4H, $J = 6.9 \text{ Hz}$), 8.44 (s, 4H), 7.67 (d, 8H, $J = 8.2 \text{ Hz}$), 5.80 (s, 8H). ^{13}C NMR (100 MHz, CD_3CN): δ 154.28 (s), 150.98 (s), 144.87 (s), 135.89 (s), 130.38 (s), 127.27 (s), 126.20 (s), 117.44 (s), 64.34 (s). HRMS (ESI): m/z calcd. for $(\text{C}_{44}\text{H}_{36}\text{F}_{12}\text{N}_8\text{P}_2)^{2+} [(\text{M}-2\text{PF}_6)/2]^+$, 483.1172; found, 483.1162.

Other compounds were synthesized using the method described in the Supporting information. The spectra of all

compounds were also deposited in Supporting information. The crystallographic data of anthracene $\text{C}1$ and pyrene $\text{C}1$ (CCDC 1508889 and 1508890, respectively) can be obtained in Supporting information and free of charge from the Cambridge Crystallographic Data Centre via www.ccdc.cam.ac.uk/data_request/cif.

Acknowledgments

We gratefully acknowledge the financial support of NNSF of China (Nos. 21402069 and 21361011) and the Project of Jiangxi Provincial Education Department (No. GJJ14264).

Appendix A. Supplementary data

Supplementary data associated with this article can be found, in the online version, at <http://dx.doi.org/10.1016/j.ccllet.2016.12.002>.

References

- (a) Z.J. Zhang, H.Y. Zhang, H. Wang, Y. Liu, A twin-axial hetero[7]rotaxane, *Angew. Chem. Int. Ed.* 50 (2011) 10834–10838;
(b) V.N. Vukotic, K.J. Harris, K. Zhu, R.W. Schurko, S.J. Loeb, Metal-organic frameworks with dynamic interlocked components, *Nat. Chem.* 4 (2012) 456–460;
(c) D.A. Leigh, V. Marcos, M.R. Wilson, Rotaxane catalysts, *ACS Catal.* 4 (2014) 4490–4497;
(d) Z. Meng, Y. Han, L.N. Wang, et al., Stepwise motion in a multivalent [2](3) catenane, *J. Am. Chem. Soc.* 137 (2015) 9739–9745;
(e) Y. Wang, G. Ping, C. Li, Efficient complexation between pillar[5]arenes and neutral guests: from host–guest chemistry to functional materials, *Chem. Commun.* 52 (2016) 9858–9872.
- M. Xue, Y. Yang, X. Chi, X. Yan, F. Huang, Development of pseudorotaxanes and rotaxanes: from synthesis to stimuli-responsive motions to applications, *Chem. Rev.* 115 (2015) 7398–7501.
- (a) B. Odell, M.V. Reddington, A.M.Z. Slawin, et al., Cyclobis(paraquat-p-phenylene): a tetracationic multipurpose receptor, *Angew. Chem. Int. Ed.* 27 (1988) 1547–1550;
(b) M. Liu, S. Li, M. Zhang, et al., Three-dimensional bis(m-phenylene)-32-crown-10-based cryptand/paraquat catenanes, *Org. Biomol. Chem.* 7 (2009) 1288–1291;
(c) H.Y. Gong, B.M. Rambo, E. Karnas, V.M. Lynch, J.L. Sessler, A ‘texas-sized’ molecular box that forms an anion-induced supramolecular necklace, *Nat. Chem.* 2 (2010) 406–409;
(d) J. Cao, H.Y. Lu, J.F. Xiang, C.F. Chen, Complexation between pentiptycene-based mono(crown ether)s and tetracationic cyclobis(paraquat-p-phenylene): who is the host or the guest? *Chem. Commun.* 46 (2010) 3586–3588;
(e) K.D. Zhang, X. Zhao, G.T. Wang, et al., Foldamer-tuned switching kinetics and metastability of [2]rotaxanes, *Angew. Chem. Int. Ed.* 50 (2011) 9866–9870;
(f) J.C. Barnes, M. Juríček, N.L. Strutt, et al., ExBox: a polycyclic aromatic hydrocarbon scavenger, *J. Am. Chem. Soc.* 135 (2013) 183–192;
(g) E.J. Dale, N.A. Vermeulen, M. Juríček, et al., Supramolecular explorations: exhibiting the extent of extended cationic cyclophanes, *Acc. Chem. Res.* 49 (2016) 262–273.
- S.T.J. Ryan, R.M. Young, J.J. Henkelis, et al., Energy and electron transfer dynamics within a series of perylene diimide/cyclophane systems, *J. Am. Chem. Soc.* 137 (2015) 15299–15307.
- (a) H.Y. Gong, B.M. Rambo, E. Karnas, et al., Environmentally responsive threading, dethreading, and fixation of anion-induced pseudorotaxanes, *J. Am. Chem. Soc.* 133 (2011) 1526–1533;
(b) H. Zhou, Z. Wang, C. Gao, J. You, G. Gao, Synthesis and characterization of a luminescent and fully rigid tetrakisimidazolium macrocycle, *Chem. Commun.* 49 (2013) 1832–1834;
(c) J.J. Henkelis, A.K. Blackburn, E.J. Dale, et al., Allosteric modulation of substrate binding within a tetracationic molecular receptor, *J. Am. Chem. Soc.* 137 (2015) 13252–13255.
- H. Bakkali, C. Marie, A. Ly, et al., Functionalized 2,5-dipyridinylpyrroles by electrochemical reduction of 3,6-dipyridinylpyridazine precursors, *Eur. J. Org. Chem.* 12 (2008) 2156–2166.
- (a) F.G. Gatti, D.A. Leigh, S.A. Nepogodiev, et al., Stiff, and sticky in the right places: the dramatic influence of preorganizing guest binding sites on the hydrogen bond-directed assembly of rotaxanes, *J. Am. Chem. Soc.* 123 (2001) 5983–5989;
(b) V. Aucagne, K.D. Hänni, D.A. Leigh, P.J. Lusby, D.B. Walker, Catalytic ‘click’ rotaxanes: a substoichiometric metal-template pathway to mechanically interlocked architectures, *J. Am. Chem. Soc.* 128 (2006) 2186–2187;
(c) C. Ke, R.A. Smaldone, T. Kikuchi, et al., Quantitative emergence of hetero[4] rotaxanes by template-directed click chemistry, *Angew. Chem. Int. Ed.* 52 (2013) 381–387.
- D.M. Bailey, A. Hennig, V.D. Uzunova, W.M. Nau, Supramolecular tandem enzyme assays for multiparameter sensor arrays and enantiomeric excess determination of amino acids, *Chem. Eur. J.* 14 (2008) 6069–6077.
- (a) D.J. Hoffart, J. Tiburcio, A. de La Torre, L.K. Knight, S.J. Loeb, Cooperative ion-ion interactions in the formation of interpenetrated molecules, *Angew. Chem. Int. Ed.* 47 (2008) 97–101;
(b) H. Chen, J. Fan, X. Hu, et al., Biphen[*n*]arenes, *Chem. Sci.* 6 (2015) 197–202;
(c) Y.M. Zhang, Z. Wang, L. Chen, H.B. Song, Y. Liu, Thermodynamics and structures of complexation between tetrasulfonated 1,5-dinaphtho-38-crown-10 and diquatery salts in aqueous solution, *J. Phys. Chem. B* 118 (2014) 2433–2441;
(d) H. Li, D.X. Chen, Y.L. Sun, et al., Viologen-mediated assembly of and sensing with carboxylatopillar[5]arene-modified gold nanoparticles, *J. Am. Chem. Soc.* 135 (2013) 1570–1576;
(e) J. Ma, Q. Meng, X. Hu, et al., Synthesis of a water-soluble carboxylatobiphen[4]arene and its selective complexation toward acetylcholine, *Org. Lett.* 18 (2016) 5740–5743.
- O.Š. Miljanić, J.F. Stoddart, Dynamic donor–acceptor [2]catenanes, *Proc. Natl. Acad. Sci. U. S. A.* 104 (2007) 12966–12970.
- B.M. Rambo, H.Y. Gong, M. Oh, J.L. Sessler, The ‘texas-sized’ molecular box: a versatile building block for the construction of anion-directed mechanically interlocked structures, *Acc. Chem. Res.* 45 (2012) 1390–1401.
- (a) C. Zhang, S. Li, J. Zhang, et al., Benzo-21-crown-7/secondary dialkylammonium salt [2]pseudorotaxane and [2]rotaxane-type threaded structures, *Org. Lett.* 9 (2007) 5553–5556;
(b) W. Jiang, H.D.F. Winkler, C.A. Schalley, Integrative self-sorting: construction of a cascade-stoppered hetero [3]rotaxane, *J. Am. Chem. Soc.* 130 (2008) 13852–13853;
(c) Q. Jiang, H.Y. Zhang, M. Han, Z.J. Ding, Y. Liu, pH-controlled intramolecular charge-transfer behavior in bistable [3]rotaxane, *Org. Lett.* 12 (2010) 1728–1731;
(d) D.H. Qu, H. Tian, Novel and efficient templates for assembly of rotaxanes and catenanes, *Chem. Sci.* 2 (2011) 1011–1015;
(e) L. Liu, Y. Liu, P. Liu, et al., Phosphine oxide functional group based three-station molecular shuttle, *Chem. Sci.* 4 (2013) 1701–1706;
(f) H. Wang, Z.J. Zhang, H.Y. Zhang, Y. Liu, Synthesis of a bistable [3]rotaxane and its pH-controlled intramolecular charge-transfer behavior, *Chin. Chem. Lett.* 24 (2013) 563–567;
(g) X. Wang, K. Han, J. Li, X. Jia, C. Li, Pillar[5]arene–neutral guest recognition based supramolecular alternating copolymer containing [c2]daisy chain and bis-pillar[5]arene units, *Polym. Chem.* 4 (2013) 3998–4003.